

International Journal of Biological Macromolecules

Computationally enhanced X-ray diffraction analysis of a gold(III) complex interacting with the human telomeric DNA G-quadruplex. Unravelling non-unique ligand positioning

--Manuscript Draft--

Manuscript Number:	
Article Type:	Research Paper
Section/Category:	Proteins and Nucleic acids
Keywords:	DNA G-quadruplex; X-ray quantum refinement; gold complexes
Corresponding Author:	Carla Bazzicalupi University of Florence: Dept. of Chemistry ITALY
First Author:	Damiani Cirri
Order of Authors:	Damiani Cirri Carla Bazzicalupi Ulf Ryde Justin Bergmann Francesca Binacchi Alessio Nocentini Alessandro Pratesi Paola Gratteri Luigi Messori
Abstract:	<p>We report on an innovative approach based on joint molecular mechanical (MM)/quantum mechanical (QM) calculations that is used to improve crystallographic solution and refinement procedures. In the here obtained crystal structure, the novel [AuL] species (with L = 2,4,6-tris(2-pyrimidyl)-1,3,5-triazine - TPymT-α) was found to be selectively bound to the human telomeric DNA Tel24 G-quadruplex (Tel24 = TAG₃(T₂AG₃)₃T) in four equally occupied conformations. The four positions of the crystallized [AuL] species were first determined by docking restrained to the crystallographically determined metal ions' coordinates. The conformations were subsequently refined by the quantum refinement method (crystallographic refinement enhanced with quantum mechanical calculation). The applied method enabled us to resolve the poorly defined density around the ligands. The occurrence of interaction in solution with the Tel24 G-quadruplex DNA was further proved through DNA melting experiments, which showed a slight destabilisation of the quadruplex upon adduct formation.</p>
Suggested Reviewers:	Michael J Hannon m.j.hannon@bham.ac.uk Kenneth Merz merz@chemistry.msu.edu Lung Wa Chung oscarchung@sustech.edu.cn Antonio Randazzo antonio.randazzo@unina.it Sylvestre Bonnet bonnet@chem.leidenuniv.nl Ya-Wen Hsiao ya-wen.hsiao@stfc.ac.uk

Opposed Reviewers:	
---------------------------	--



UNIVERSITÀ
DEGLI STUDI
FIRENZE

DIPARTIMENTO
DI CHIMICA
"UGO SCHIFF"

Manuscript: Computationally enhanced X-ray diffraction analysis of a gold(III) complex interacting with the human telomeric DNA G-quadruplex. Unravelling non-unique ligand positioning

Dear Editor,

I am submitting the above manuscript that I would like you to consider for publication in *International Journal of Biological Macromolecules* as an Article.

It describes the new crystal structure of the Human Telomeric DNA in complex with a mononuclear gold(III) complex.

Among the numerous identified Putative Quadruplex Sequences, relevant in the human genome, G-quadruplexes formed by the telomeric DNA sequence play a leading role, due to their ability to inhibit the Telomerase enzyme's activity in malignant cell. In this context, structural information of the binding features of this target are of primary importance, but achieving this information is very often made difficult, or even impossible, due to intrinsic structural disorder.

The structure we report here has been solved by an innovative approach based on MM/QM enhanced crystallographic refinement, specifically developed to take in to account structural disorder. This method enabled us to localize the crystallized metal complex spread over four different positions in the binding site, obtaining a good quality crystal structure from an intrinsically disordered sample.

As a result of this process, we describe here the binding features of the adduct formed by the human telomeric DNA G-quadruplex and a newly synthesized gold(III) complex. The interest in metal complexes as quadruplex binders is rapidly growing as they can represent a valid alternative in the search for small molecules with therapeutic and/or diagnostic purposes.

For these reasons, we believe that this manuscript is of enough general interest, novelty and impact to deserve consideration for publication in *International Journal of Biological Macromolecules*.

Thank you in advance.

Sincerely Yours,

Carla Bazzicalupi

Computationally enhanced X-ray diffraction analysis of a gold(III) complex interacting with the human telomeric DNA G-quadruplex. Unravelling non-unique ligand positioning

Damiano Cirri^a, Carla Bazzicalupi^{b,*}, Ulf Ryde^{c,*}, Justin Bergmann^c, Francesca Binacchi^a, Alessio Nocentini^d, Alessandro Pratesi^a, Paola Gratteri^{d,*}, Luigi Messori^b

^a Department of Chemistry and Industrial Chemistry, University of Pisa, Via G. Moruzzi 13, 56124 Pisa, Italy.

^b Department of Chemistry “Ugo Schiff”, University of Florence, Via della Lastruccia 3-13, 50019 Sesto Fiorentino, Italy.

^c Division of Theoretical Chemistry, Lund University, Chemical Centre, P. O. Box 124, SE-221 00 Lund, Sweden

^d Department NEUROFARBA – Pharmaceutical and Nutraceutical Section and Laboratory of Molecular Modeling Cheminformatics & QSAR, University of Florence, Via U. Schiff 6, 50019 Sesto Fiorentino, Florence, Italy.

Corresponding authors: Carla Bazzicalupi (carla.bazzicalupi@unifi.it), Ulf Ryde (ulf.ryde@teokem.lu.se), Paola Gratteri (paola.gratteri@unifi.it)

Abstract

We report on an innovative approach based on joint molecular mechanical (MM)/quantum mechanical (QM) calculations that is used to improve crystallographic solution and refinement procedures. In the here obtained crystal structure, the novel [AuL] species (with L = 2,4,6-tris(2-pyrimidyl)-1,3,5-triazine - TPymT- α) was found to be selectively bound to the human telomeric DNA Tel24 G-quadruplex (Tel24 = TAG₃(T₂AG₃)₃T) in four equally occupied conformations. The four positions of the crystallized [AuL] species were first determined by docking restrained to the

crystallographically determined metal ions' coordinates. The conformations were subsequently refined by the quantum refinement method (crystallographic refinement enhanced with quantum mechanical calculation). The applied method enabled us to resolve the poorly defined density around the ligands. The occurrence of interaction in solution with the Tel24 G-quadruplex DNA was further proved through DNA melting experiments, which showed a slight destabilisation of the quadruplex upon adduct formation.

1
2
3
4 **Computationally enhanced X-ray diffraction analysis of a**
5 **gold(III) complex interacting with the human telomeric DNA**
6
7 **G-quadruplex. Unravelling non-unique ligand positioning**
8
9

10 Damiano Cirri^a, Carla Bazzicalupi^{b,*}, Ulf Ryde^{c,*}, Justin Bergmann^c, Francesca

11 Binacchi^a, Alessio Nocentini^d, Alessandro Pratesi^a, Paola Gratteri^{d,*}, Luigi Messori^b
12
13

14
15
16 a Department of Chemistry and Industrial Chemistry, University of Pisa, Via G. Moruzzi 13, 56124
17
18 Pisa, Italy.
19

20
21 b Department of Chemistry “Ugo Schiff”, University of Florence, Via della Lastruccia 3-13, 50019
22
23 Sesto Fiorentino, Italy.
24

25
26 c Division of Theoretical Chemistry, Lund University, Chemical Centre, P. O. Box 124, SE-221 00
27
28 Lund, Sweden
29

30
31 d Department NEUROFARBA – Pharmaceutical and Nutraceutical Section and Laboratory of
32
33 Molecular Modeling Cheminformatics & QSAR, University of Florence, Via U. Schiff 6, 50019 Sesto
34
35 Fiorentino, Florence, Italy.
36

37
38 Corresponding authors: Carla Bazzicalupi (carla.bazzicalupi@unifi.it), Ulf Ryde
39
40 (ulf.ryde@teokem.lu.se), Paola Gratteri (paola.gratteri@unifi.it)
41
42
43
44
45
46
47
48
49
50
51
52
53
54
55
56
57
58
59
60
61
62
63
64
65

Abstract

We report on an innovative approach based on joint molecular mechanical (MM)/quantum mechanical (QM) calculations that is used to improve crystallographic solution and refinement procedures. In the here obtained crystal structure, the novel [AuL] species (with L = 2,4,6-tris(2-pyrimidyl)-1,3,5-triazine - TPymT- α) was found to be selectively bound to the human telomeric DNA Tel24 G-quadruplex (Tel24 = TAG₃(T₂AG₃)₃T) in four equally occupied conformations. The four positions of the crystallized [AuL] species were first determined by docking restrained to the crystallographically determined metal ions' coordinates. The conformations were subsequently refined by the quantum refinement method (crystallographic refinement enhanced with quantum mechanical calculation). The applied method enabled us to resolve the poorly defined density around the ligands. The occurrence of interaction in solution with the Tel24 G-quadruplex DNA was further proved through DNA melting experiments, which showed a slight destabilisation of the quadruplex upon adduct formation.

Keywords:

X-ray diffraction, QM/MM, DNA G-quadruplex, gold complexes, quantum refinement, melting experiments

1. Introduction

In the last decades, the guanine quadruplex (G4) non-canonical folding [1] has been recognized as an important element in the control of essential biological processes such as oncogenesis, infectious protein control, parasitic and neurodegenerative mechanisms [2]. Compared to the very large number of identified Putative Quadruplex Sequences (PQSs – estimated to be ~376,000 in the human genome) [3], up to now only few of them are known to have biologically relevant functions. Among them, G-quadruplexes that can be formed at the telomeric end of eukaryotic human chromosomes attract much interest, as they were found to inhibit the telomerase-based cell immortalization mechanism, present in about 85% of cancer diseases [4]. Hence, the need for small molecules of therapeutic and/or diagnostic interest, able to bind or even to promote human telomeric G4 formation has remarkably grown. In this context, metal complexes [5] can represent an interesting alternative to the more explored organic ligands [6], due to the variability deriving from the efficient metal driven assembly of building blocks with potentially diverse features. In addition, the positive charge of the metal centres conveniently complements the anionic nature of the nucleic acids.

Despite the growing interest in medicinal applications of transition metal complexes, very little structural information is available in the literature concerning the binding of metal complexes to G4s. Indeed, among the numerous references published during the last ten years [7], only ten papers report structures solved in atomic detail by X-ray diffraction (Protein Data Bank (pdb) [8] codes: 3QSC, 3QSF, 5CCW, 5LS8, 6H5R, 6RNL, 6XCL) or solution NMR techniques (pdb codes: 2MCC, 2MCO, 5MVB, 5Z8F, 5Z80, 6LNZ).

Notably, most of these studies concern platinum or gold complexes, most likely because these metals are intensely studied due to their large anticancer potential (cf. cisplatin and its analogues carboplatin and oxaliplatin, which are in widespread clinical use) [9]. Gold-containing compounds attract attention also for their antimicrobial or antiparasitic activities [10]. In addition, the electronic configurations, associated with the common oxidation states of both elements, typically lead to

1 square-planar ($d^8 - \text{Pt}^{2+}$ and Au^{3+}) or linear geometries ($d^{10} - \text{Au}^+$), which favour DNA binding
2 through either intercalation or external stacking.
3

4 With this in mind, we started considering the possibility of using platinum(II) and gold(III) complexes
5 of the TPymT- α ligand for medicinal applications (Fig 1). TPymT- α shows peculiar and unique
6 coordination chemistry properties: this ligand can in principle coordinate up to three metal ions at
7 identical sites through a N3 donor set. However, only a limited number of studies employing this
8 ligand have appeared so far owing to its generally poor solubility in common solvents and to the
9 facile hydrolysis of the central triazine fragment [11].
10
11
12
13
14
15
16
17
18

19 In principle, the TPymT- α ligand is expected to give polynuclear Pt(II) and Au(III) complexes, each
20 featuring a wide positively charged planar surface with aromatic character. These structural
21 characteristics are known to favour binding toward nucleic acid structures, both in double helix and
22 in G-quadruplex (G4) folding. Our efforts were first directed to the synthesis of the corresponding Pt
23 complexes, and we succeeded in obtaining the $[\text{Pt}_3(\text{TpymT})\text{Cl}_3]^{3+}$ species bearing three platinum
24 cations coordinated by the N3 donor cavities and a chloride ligand as the fourth ligand, with three
25 hydroxide anions as counterions [12].
26
27
28
29
30
31
32
33
34
35

36 However, solution studies revealed the occurrence of a non-intercalative interaction toward calf
37 thymus DNA in the double helix B form, with a preferential external/groove binding [12]. As this
38 behavior can be the likely result of a poor match between the wide triplatinum complex and the
39 intercalative binding site of the DNA B-form, we decided to check the binding ability of different
40 TpymT- α metal complexes toward G4.
41
42
43
44
45
46
47

48 Accordingly, we have carried out the reaction of the TpymT- α ligand with HAuCl_4 and characterised
49 the resulting products (Figure 1). Afterwards, CD-melting experiments and crystallization screening
50 were carried out to characterize the interaction of the obtained gold compounds with a 24-mer human
51 telomeric DNA in quadruplex folding. One X-ray data set was good enough to solve the crystal
52 structure of the human Tel24 G-quadruplex (Tel24 = TAG₃(T₂AG₃)₃T) in complex with the
53
54
55
56
57
58
59
60
61
62
63
64
65

1 mononuclear [(TpymT- α)AuCl]²⁺ species, but refinement was difficult owing to the non-unique
2 positioning of the complex on the guanine tetrad.
3

4 This kind of issue has been previously reported for several G4/ligand X-ray and NMR structures [13],
5 and appears particularly important for metal complexes in square-planar or linear coordination
6 geometries [14-16]. In order to better resolve this disorder issue and obtain a more certain and clear
7 picture of the overall binding site for [(TpymT- α)AuCl]²⁺, we decided to test the reliability of the
8 quantum refinement method, i.e. crystallographic refinement enhanced with QM calculations, which
9 has been successfully applied to resolve issues in protein structures with a poor density around the
10 metal atoms [17].
11
12
13
14
15
16
17
18
19
20

21 In the present study, an innovative approach based on (joint molecular mechanical (MM)/quantum
22 mechanical (QM) calculations was used to improve the crystallographic refinement for the adduct
23 formed by Tel24 with [(TpymT- α)AuCl]²⁺, where the metal complex in the binding site is spread
24 over four symmetry non-equivalent positions.
25
26
27
28
29
30

31 **2. Experimental**

32 **2.1. Materials**

33
34
35
36
37
38 The human telomeric DNA sequence d[TAG₃(T₂AG₃)₃T] (Tel24) was purchased from Jena
39 Bioscience as lyophilized material. Analytical grade reagents and ultra-pure water obtained through
40 a Millipore S.A.670120 Mosheim apparatus were employed.
41
42
43
44

45 **2.2 Synthesis**

46
47
48 In a 50 mL flask, 5 mL of EtOH, 88 mg (0.28 mmol) of TpymT- α ligand and 1.7 mL of an aqueous
49 solution of H₂AuCl₄ (339.8 mg/mL) were added. Subsequently, 82 mg of NaHCO₃ were added and
50 the resulting mixture was stirred at 55 °C. After 2 h, the suspension was dried under reduced pressure
51 and the remaining solid was suspended in 1.5 mL of H₂O. The suspension was filtered of a sintered
52 glass funnel and the collected yellow solid was washed with water, diethyl ether and dried at reduced
53 pressure. After desiccation, 188 mg of product (**I**) were collected.
54
55
56
57
58
59
60
61
62
63
64
65

2.3 DNA melting experiments

A UV-2450 SHIMADZU double-beam UV-vis spectrophotometer (Kyoto, Japan) was used for melting experiments. The instrument has a jacketed cell holder providing temperature control within ± 0.1 °C. To avoid signal saturation, all spectra were recorded using 500 μ L quartz cuvettes with an optical path of 2 mm. The thermal denaturation curves of Tel-24 G-quadruplex (G4) samples containing the investigated product (**I**) or the TPymT- α ligand, in a 1:3 molar ratio, were measured at increasing temperatures ranging from 25 °C to 65 °C following the absorbance changes at 290 nm. All the experiments were performed in 0.1 M ammonium acetate solution, pH 7.0. The percentage of absorbance change was plotted against temperature and defined as follows:

$$\%A \text{ change} = 100 \times (A(T) - A^\circ) / (A^\infty - A^\circ)$$

where $A(T)$ is the absorbance read at each temperature T (°C), A° the absorbance corresponding to the initial plateau and A^∞ the absorbance of the final plateau. In this way, a sigmoidal curve could be obtained. The melting temperature was calculated as the maximum of the first derivative of the sigmoidal curve.

2.4 Computationally enhanced X-ray diffraction analysis

Product (**I**) was dissolved in DMSO to a total 10 mM concentration, while the Tel24 sequence was dissolved in 20 mM potassium cacodylate pH 6.5 and 50 mM KCl up to a concentration 1 mM, and annealed to allow G-quadruplex formation by heating to 90 °C for 15 min and then slowly cooling to RT overnight. The stock DMSO solution was added to the DNA annealed solution in 1:1 product (**I**):DNA molar ratio and the resulting solution was incubated at 25 °C for 20 min. Crystallization trials were set up by mixing 1 μ L DNA–drug complex solution with 1 μ L crystallization solution. Crystals of [(TpymT- α)AuCl] $^{2+}$ / Tel24 suitable to SC-XD analysis were obtained at 296 K using the sitting drop vapor diffusion method from a solution containing 20% v/v isopropanol, 50 mM potassium cacodylate pH 6.5, 50 mM Li₂SO₄, 50 mM MgSO₄, on the basis of a reported screening [18]. Drops were equilibrated against the same solution (100 μ L).

1 The [(TpymT- α)AuCl]²⁺ / Tel24 complex crystallizes in the monoclinic system, space group C2 ($a =$
2 36.78 Å, $b = 71.53$ Å, $c = 26.24$ Å, $\beta = 92.42^\circ$). Data collection was performed using synchrotron
3
4 light ($\lambda = 0.87313$ Å, ID23-1 Beamline, ESRF Grenoble). Data were collected at 100 K, using the
5
6 crystallization solution added with glycerol up to 30% v/v as cryoprotectant. Data were integrated
7
8 and scaled using the program XDS [19]. The structure was solved by the Molecular Replacement
9
10 technique using the program MOLREP [20] and the coordinates of the Tel24 G-quadruplex structure
11
12 PDB-6H5R [16], without all the heteroatoms, as a search model. The model was refined with the
13
14 program Refmac5 [21] from the CCP4 program suite [22]. Manual rebuilding of the model was
15
16 performed using the program Coot [23]. For the T24 residue, only the phosphate group was clearly
17
18 visible in the electron density map, thus only those coordinates were refined. The model obtained at
19
20 this step of refinement consisted of the overall DNA coordinates, potassium ions, and a gold ion,
21
22 spread over four sites (0.25 occupancy factor each).
23
24
25
26
27
28

29 Restrained docking calculations were carried out to obtain a preliminary positioning of the overall
30
31 ligand spread over the four sites. The model was prepared using the Protein Preparation Wizard tool
32
33 implemented in the Schrödinger suite [24]. The energy minimization protocol with a root mean square
34
35 deviation (RMSD) value of 0.30 Å was applied using the OPLS3e force field. The Au ion complex
36
37 was submitted to quantum mechanics geometry optimization (B3LYP/LACVP**+) and ESP charge
38
39 calculation with Jaguar [24a]. Standard precision (SP) docking experiments were carried out using
40
41 the software Glide [24b] and the QM charges. Four grids were prepared, each centred on one of the
42
43 Au³⁺ ions. A positional constraint for the ligand was set on the Au³⁺ ion to be docked within 0.5 Å of
44
45 the metal ion position detected experimentally. The highest docking score criterion was used to select
46
47 a single pose per gold ion out of a maximum of five docking outcomes.
48
49
50
51
52

53 The docked structure was then used as the starting structure for quantum refinement [17a,b]. Quantum
54
55 refinement is standard crystallographic refinement in which the empirical restraints (used to ensure
56
57 that the final structure gives reasonable bond lengths and angles) are replaced by more accurate
58
59 quantum mechanical (QM) calculations for a small, but interesting part of the structure. This approach
60
61
62
63
64
65

1 was recently extended to allow for multiple conformations in the QM system [17c]. In the present
2 study, it was further extended to four conformations in the QM system, by simply performing four
3
4 separate QM calculations for each conformation. Further details of the implementation are given in
5
6 the ESI. The calculations were performed with the ComQum-X software [17a], which is a
7
8 combination of Turbomole [25] and the crystallography and NMR system (CNS), version 1.3 [26].
9
10 The full Tel24 G-quadruplex was used in all calculations, including all crystal-water molecules. For
11
12 the DNA, we used the standard CNS force field (dna-rna_rep.param, water_rep.param and
13
14 ion.param). The w_A factor (determining the relative weight between the crystallographic data and the
15
16 empirical potential, cf. Eqn. 2 in the ESI) was the default value suggested by CNS, 4.153. The w_{MM}
17
18 weight was set to 1/3 as in all our previous studies [17a,c]. For the crystallographic target function,
19
20 we used the standard maximum-likelihood function using amplitudes (mlf) in CNS [27].
21
22
23
24

25
26 The QM system involved four copies of the (TpymT- α)AuCl complex (we tested also OH⁻ instead of
27
28 Cl⁻ coordinated to the Au ion, but the fit to the crystallographic data was worse). Calculations were
29
30 performed for the triplet and (closed-shell) singlet states, but the singlet was found to be lowest in
31
32 energy by ~60 kJ/mol and will only be discussed in the following. The QM calculations were
33
34 performed at the TPSS/def2-SV(P) level of theory (including a 60-electron relativistic effective core
35
36 potential for Au) [28]. The calculations were sped up by expanding the Coulomb interactions in an
37
38 auxiliary basis set, the resolution-of-identity (RI) approximation [29]. Empirical dispersion
39
40 corrections were included with the DFT-D3 approach [30] and Becke–Johnson damping [31].
41
42
43
44

45 Finally, a few refinement cycles were performed with the software Refmac5 [21] in order to obtain
46
47 final refinement statistics. These values as well data collection information are reported in Table S2,
48
49 supporting information.† Final coordinates and structure factors have been deposited with the Protein
50
51 Data Bank (PDB accession number 7QVQ).
52
53

54 55 **3. Results and Discussion**

56 57 58 **3.1 Synthesis of gold(III) complexes of the TpymT- α ligand**

59
60
61
62
63
64
65

1
2
3
4
5
6
7
8
9
10
11
12
13
14
15
16
17
18
19
20
21
22
23
24
25
26
27
28
29
30
31
32
33
34
35
36
37
38
39
40
41
42
43
44
45
46
47
48
49
50
51
52
53
54
55
56
57
58
59
60
61
62
63
64
65

By analogy with the previously synthesised $[\text{Pt}_3(\text{TpymT})\text{Cl}_3]^{3+}$ complex we aimed to prepare the corresponding trinuclear complex where three gold atoms are coordinated by the TpymT- α ligand. Thus, the TpymT- α ligand was reacted with an excess of tetrachloroauric acid and a solid product obtained as described in the experimental section. The obtained product (**I**) was subsequently characterized by a variety of biophysical methods including ^1H NMR, IR spectroscopy, and elemental analysis. Based on these analytical determinations, we realized that the obtained product is indeed a mixture of two main species, i.e. $[\text{Au}_2\text{L}]$ and $[\text{AuL}]$ (charges and coordinated anions omitted here and in the following). More precisely, the CHN analysis suggested that the two species $[(\text{TpymT}-\alpha)\text{AuCl}]\text{Cl}_2$ and $[(\text{TpymT}-\alpha)\text{Au}_2\text{Cl}_2]\text{Cl}_4$ (Table S1 – supporting material) are present in nearly equal amounts.

Unfortunately, all attempts to separate the two species $[(\text{TpymT}-\alpha)\text{AuCl}]\text{Cl}_2$ and $[(\text{TpymT}-\alpha)\text{Au}_2\text{Cl}_2]\text{Cl}_4$ failed. For this reason, the whole mixture was used as such for the subsequent studies. From the inspection of the IR spectrum of (**I**) (see Figure S1 in supporting material), three main bands were detected at 358 cm^{-1} , 318 cm^{-1} , and 230 cm^{-1} attributable to the Au-Cl, N-Au-Cl and Au-N modes, respectively [32] providing additional evidence for the presence of chloride as the fourth ligand of the gold(III) center. Product (**I**) is poorly soluble in water, while manifesting a greater solubility in DMSO.

3.2 DNA melting experiments

Spurred by the aforementioned evidence and upon considering the ligand structure and the likely planar structure of the gold(III) complexes contained in the product (**I**), we started investigating the interaction of this product with the Tel24 G-quadruplex that is known to manifest a preference for planar compounds containing aromatic groups. DNA melting studies were first performed to demonstrate the occurrence of a sufficiently tight interaction in solution. Tel24 G-quadruplex and the product (**I**) or the TpymT- α ligand were thus reacted at room temperature in a molar ratio $C_{\text{product}}(\text{I})/C_{\text{G4}} = C_{\text{ligand}}/C_{\text{G4}} = 3$. An excess of the reactive molecules with respect to the DNA structure was

1 used both to ensure a sufficient amount of the possible formed adducts that could be observed by this
2 analysis, and also to provide a suitable amount of the reacting molecule for all the possible
3 biomolecule's binding sites. Results of the melting experiments are shown in Figure 2 and in Table
4 S3. From inspection of these data, it emerges that product (**I**) is able to significantly modify the
5 melting profile of the Tel24 G quadruplex. In detail, binding of (**I**) results in a small but clear
6 destabilisation of the Tel24 G quadruplex by around 2 °C. We interpret this decrease of the melting
7 temperature as the indication of the occurrence of a direct interaction between the Tel24 G quadruplex
8 and product (**I**).
9
10
11
12
13
14
15
16
17
18

19 **3.2 Computationally enhanced X-ray diffraction analysis**

20 Crystals suitable for X-ray diffraction analysis were obtained upon incubation of the telomeric DNA
21 sequence Tel24 with the product (**I**) under the crystallization conditions described in the Experimental
22 section. The electron density map clearly shows monomolecular DNA G-quadruplexes arranged in
23 columns growing along the c axis (Figure 3a). The G4 structures assume the expected all parallel
24 conformation, characterized by three stacked G-tetrads at 3.4 Å inter-planar distance, and potassium
25 ions in the internal channel (2.6–3.1 Å apart from the guanine O6 atoms). In each column, pairs of
26 G4 units, symmetry-related by two-fold rotation axis, stack on one another forming dimers stabilized
27 by the presence of a potassium ion at the interface between 5'-end G-tetrads in each couple of adjacent
28 quadruplexes.
29
30
31
32
33
34
35
36
37
38
39
40
41
42
43

44 Similar G4 couples, stabilized by potassium [8,14,33] or strontium ions [16], have previously been
45 reported. The G4 dimers expose their 3'-end guanine tetrads, which constitute the ligand binding site.
46 Actually, the 3'-end G-tetrads from symmetry-related dimers repeating along the c axis, lie about 10
47 Å apart from one another. In the resulting cavity, eight prominent peaks were evident in the electron
48 density map, which can be split in two groups and overall assigned to two symmetry-related gold
49 ions, each spread over four almost coplanar positions. A similar disordered binding mode was
50 previously found for the bis carbene gold(I) complex $[\text{Au}(\text{1-butyl-3-methyl-2-ylidene})_2]^+$ in adduct
51 with a propeller telomeric quadruplex [16], where two symmetry-related disordered gold complexes,
52
53
54
55
56
57
58
59
60
61
62
63
64
65

1 each spread over four approximately coplanar positions, were suggested to be present in the binding
2 site.
3

4 Since the product (**I**) is an almost equimolar mixture of mononuclear [(TpymT- α)AuCl]Cl₂ and
5 binuclear [(TpymT- α)Au₂Cl₂]Cl₄, we have to take into account the possibility that the mononuclear
6 complex alone, the binuclear one or a combination of the two could have been cocrystallized with the
7 DNA. An investigation of the Cambridge Structural Database [34] revealed that in the bi- and
8 trinuclear complexes of TpymT- α , containing second- or third-row transition metal ions,
9 intramolecular intermetallic distances are 6.5–7 Å. This data led us to eliminate the hypothesis that
10 only the binuclear complex could have been cocrystallized with DNA. In fact, among the three longest
11 inter-metallic distances between the four coplanar gold ions in the crystal structure of the binding site
12 (about 5, 6 and 7 Å), only one of them is compatible with the expected intramolecular intra-gold
13 distance of a binuclear complex. On the other hand, the hypothesis of a mixture of [(TpymT-
14 α)AuCl]/DNA and [(TpymT- α)Au₂Cl₂]/DNA in 2:1 molar ratio was discarded, as almost the same
15 amount of electrons was associated to each of the four peaks, leading to equally populated gold
16 positions. Thus, two symmetry-related mononuclear gold complexes, each one spread over four
17 approximately coplanar positions, seem to fit the crystallographic data best.
18
19
20
21
22
23
24
25
26
27
28
29
30
31
32
33
34
35
36
37
38

39 Unfortunately, the residual electron density did not allow a clear localization of the lighter atoms (C
40 and N). Thus, the four metal complexes in the asymmetric unit were firstly located on the 3'-end
41 tetrad by molecular docking and then refined, with fractional occupation factors (0.25), against the
42 observed structure factors by the ComQumX-4QM method [17]. The QM calculations ensure
43 chemically reasonable structures of the (TpymT- α)AuCl complexes and provide structures that are
44 an optimal compromise between the crystallographic raw data and the QM calculations. The resulting
45 structures are shown in Figure 3b-e and in Figure S2 and S3, supporting material. Each [(TpymT-
46 α)AuCl] molecule is found at π - π stacking distance from the nearest 3'-end G-tetrad (3.3 Å), and at
47
48
49
50
51
52
53
54
55
56
57
58
59
60
61
62
63
64
65

1 even closer interplanar distance (about 3.1 Å) from the symmetry-related [(TpymT- α)AuCl]
2 molecules (Figure S2).
3

4
5 As shown in Figure 3, the TpymT- α moieties match the guanine tetrad well. In [(TpymT- α)AuCl]-C
6 (Figure 3b), [(TpymT- α)AuCl]-E (Figure 3d) and [(TpymT- α)AuCl]-F (Figure 3e), the triazine ring
7 is placed over the G4 central channel, and all the three pyrimidine rings give π -stacking interaction
8 with an equivalent number of guanine residues. The gold(III) metal ion is placed in close proximity
9 (3.4–3.7 Å) to the carbonyl oxygen and the N7 nitrogen of G5 and G11 ([[(TpymT- α)AuCl]-C and
10 [(TpymT- α)AuCl]-E, respectively), or to the O6 and N7, and the N1 and N2 heteroatoms of G23 and
11 G17, respectively ([[(TpymT- α)AuCl]-F). The position of the fourth complex ([[(TpymT- α)AuCl]-D,
12 Figure 3c) shows distinct binding features, with the gold center placed above the potassium channel.
13 The π -stacking interaction involves mainly a pyrimidine group and the triazine unit of the ligand, and
14 only two guanines in the 3'-end tetrad (G5 and G11). The non-coordinated pyrimidine is placed above
15 the G11 ribose, giving a slight loss of planarity of the overall TpymT- α moiety. No water molecules
16 were found in the binding site at contact distance with the coordinated chloride or the free pyrimidine
17 nitrogens.
18
19

20 Thus, despite the disorder affecting the binding site, in our opinion this crystal structure evidences
21 the binding preferences of Au(III)-TpymT- α toward the telomeric G-quadruplexes, as in three out of
22 four observed ligand positions, the metallodrug gives almost the same kind of interactions. Actually,
23 the good conformational match between the three pyrimidines and the guanines residues seems to be
24 the main driving force for the binding of the Tpymt ligand, and the resulting π - π stacking provides
25 an important contribution to the stability of the adduct. Moreover, it is likely that in [(TpymT-
26 α)AuCl]-C, [(TpymT- α)AuCl]-E and [(TpymT- α)AuCl]-F (Figure 3b,d,e), triazine ring does not
27 only play the role of linker group, but it also contributes itself to the overall binding. In fact, triazine,
28 being an electron-poor heteroaromatic ring, is known to possess an inverted molecular quadrupole
29 moment compared to benzene and other electron-rich aromatic groups. The inversion of the
30
31
32
33
34
35
36
37
38
39
40
41
42
43
44
45
46
47
48
49
50
51
52
53
54
55
56
57
58
59
60
61
62
63
64
65

1 quadrupole moment is connected to the accumulation of positive charge towards the ring centre, while
2 the periphery of the ring becomes negative. This phenomenon turns the electron-poor aromatic system
3
4 into a π -acid, known to be able to give attractive interactions with anions and lone-pair bearing atoms
5
6 [35]. Notoriously, the central G-quadruplex channel is characterized by the carbonyl oxygens, locally
7
8 accumulating negative charge neutralized by the alkali ions. Thus, when placed over the G4 central
9
10 channel, triazine likely exerts an analogous charge–charge neutralizing action, thereby contributing
11
12 to the overall stabilization of the system.
13
14

15
16 In addition, interesting comparisons can be made with the gold(I) complexes, [Au(1-butyl-3-methyl-
17
18 2-ylidene)₂]⁺ and [Au(9-methylcaffeine-8-ylidene)₂]⁺, complexed with telomeric DNA quadruplex,
19
20 whose crystal structures have been previously reported [14,16]. In these structures, the gold(I) ions
21
22 are never found at the central channel, but they always interact with guanines and are placed at about
23
24 3.5 Å from N1 nitrogens. Thus, despite the high oxidation state of gold in [(TpymT- α)AuCl], which
25
26 should favour the metal ion being at the central channel, the bulky TpymT- α structure disfavours this
27
28 placement, and the binding preferences of this metallodrug are due to a combined effect of pyrimidine
29
30 stacking, metal–guanine interactions and charge–charge neutralizing actions of triazine’s inverted
31
32 quadrupole moment.
33
34
35
36
37
38

39 Conclusions

40
41
42
43 The reaction of the ligand 2,4,6-tris(2-pyrimidyl)-1,3,5-triazine (TpymT- α , L) with an excess of
44
45 tetrachloroauric acid yields a product (**I**) that turned out to be a nearly equimolar mixture of the mono
46
47 and bis gold(III) complexes [AuL] and [Au₂L]. Both these species bear tetracoordinate square planar
48
49 gold(III) centers with chloride as the fourth ligand. Melting experiments provided evidence for the
50
51 formation of an adduct between product (**I**) and human telomeric DNA Tel24 G-quadruplex.
52
53 Structural results were obtained applying crystallographic refinement enhanced with QM calculation,
54
55 which enabled us to resolve issues with poor electron density due to the spreading of the mononuclear
56
57 complex [(TpymT- α)AuCl] over four equally populated positions, stacked at the 3’-end G-tetrad of
58
59
60
61
62
63
64
65

1 the telomeric quadruplex. The structural results document the occurrence of a fishing-like
2 crystallization process, for which only the [AuL] species is selectively bound to the telomeric G-
3 quadruplex. Analysis of the obtained crystal structure revealed that the binding preferences of this
4 quadruplex. Analysis of the obtained crystal structure revealed that the binding preferences of this
5 metallodrug arise from a combined effect of pyrimidine stacking, metal–guanine interactions and
6 charge–charge neutralizing action of triazine’s inverted quadrupole moment.
7
8
9
10

11 **Acknowledgements**

12
13 The authors gratefully acknowledge Prof. Roberto Bini (LENS, University of Florence) for
14 acquisition of the IR spectrum.
15
16
17
18
19
20

21 **Fundings**

22
23 This work was supported by the Fondazione Cassa di Risparmio di Firenze (ERC, project number
24 23942.2019); the Swedish research council (grants numbers 2018-05003 and 2020-06176); the
25 eSENCE e-science collaboration; the Associazione Italiana per la Ricerca sul Cancro (AIRC, grant
26 number 23852); the University of Pisa (PRA 2020_39); the Beneficentia Stiftung (Vaduz,
27 BEN2020/34). The computations were performed on computer resources provided by the Swedish
28 National Infrastructure for Computing (SNIC) at Lunarc at Lund University and HPC2N at Umeå
29 University, partially funded by the Swedish Research Council (grant 2018-05973).
30
31
32
33
34
35
36
37
38
39
40
41

42 **Author contributions**

43
44 Damiano Cirri: Investigation, Formal analysis. Carla Bazzicalupi: Conceptualization, Formal
45 analysis, Funding acquisition; Writing – Original draft and Review and Editing, Visualization,
46 Validation. Project administration. Ulf Ryde: Formal analysis, Writing – Original draft and Review
47 and Editing, Visualization, Funding acquisition. Justin Bergmann: Investigation, Formal analysis.
48 Francesca Binacchi: Investigation, Formal analysis. Alessio Nocentini: Investigation, Formal
49 analysis. Alessandro Pratesi: Investigation, Formal analysis, Funding acquisition. Paola Gratteri:
50 Conceptualization, Formal analysis, Funding acquisition; Writing – Original draft and Review and
51
52
53
54
55
56
57
58
59
60
61
62
63
64
65

1 Editing, Visualization, Validation. Luigi Messori: Formal analysis, Investigation, Writing – Original
2 draft and Review and Editing, Visualization.
3
4

5 **References**

6
7

- 8
9 [1] D. Rhodes, H. J. Lipps, G-quadruplexes and their regulatory roles in biology, *Nucleic Acids*
10 *Res.* 43 (2015) 8627–8637. <https://doi.org/10.1093/nar/gkv862>; c) H. L. Lightfoot, T. Hagen, N. J.
11 Tatum, J. Hall, The diverse structural landscape of quadruplexes, *FEBS Letters* 593 (2019) 2083–
12 2102. <https://doi.org/10.1002/1873-3468.13547>.
13
14
15
16
17 [2] a) E. Ruggiero, S. N. Richter, G-quadruplexes and G-quadruplex ligands: targets and tools in
18 antiviral therapy, *Nucleic Acids Res.* 46 (2018) 3270 – 3283. <https://doi.org/10.1093/nar/gky187>; b)
19 F. Dumetz, C. J. Merrick, Parasitic protozoa: unusual roles for G-quadruplexes in early-diverging
20 eukaryotes *Molecules* 24 (2019) 1339–1350. <https://doi.org/10.3390/molecules24071339>
21
22 [3] A.K. Todd, M. Johnston, S. Neidle, Highly prevalent putative quadruplex sequence motifs in
23 human DNA. *Nucleic Acids Res.* 33 (2005), 2901–2907. <https://doi.org/10.1093/nar/gki553>.
24
25 [4] E. Henderson, C.C. Hardin, S.K. Walk, I.Jr Tinoco, E.H. Blackburn, Telomeric DNA
26 oligonucleotides form novel intramolecular structures containing guanine-guanine base pairs, *Cell.*,
27 51 (1987) 899–908. [https://doi.org/10.1016/0092-8674\(87\)90577-0](https://doi.org/10.1016/0092-8674(87)90577-0)
28
29 [5] Q. Cao, Y. Li, E. Freisinger, P. Z. Qin, R. K. O. Siegel, Z.-W. Mao, G-quadruplex DNA
30 targeted metal complexes acting as potential anticancer drugs, *Inorg. Chem. Front.* 4, (2017), 10–
31 32. <https://doi.org/10.1039/C6QI00300A>
32
33 [6] A. R. Duarte, E. Cadoni, A. S. Ressurreição, R. Moreira, A. Paulo, Design of Modular G-
34 quadruplex Ligands, *ChemMedChem* 2018, 13, 869 –893. <https://doi.org/10.1002/cmdc.201700747>.
35
36 [7] E. Palma, J. Carvalho, C. Cruz, A. Paulo, Metal-Based G-Quadruplex Binders for Cancer
37 Theranostics, *Pharmaceuticals* 2021, 14, 605. <https://doi.org/10.3390/ph14070605>
38
39
40
41
42
43
44
45
46
47
48
49
50
51
52
53
54
55
56
57
58
59
60
61
62
63
64
65

1 [8] H. M. Berman, J. Westbrook, Z. Feng, G. Gilliland, T. N. Bhat, H. Weissig, I. N. Shindyalov, P.
2 E. Bourne, The Protein Data Bank, *Nucleic Acids Res.*, 28 (2000) 235-42.

3
4 <https://doi.org/10.1093/nar/28.1.235>.

5
6 [9] L. Massai, D. Cirri, E. Michelucci, G. Bartoli, A. Guerri, M.A. Cinellu, F. Cocco, C. Gabbiani,
7 L.Messori, Organogold(III) compounds as experimental anticancer agents: chemical and biological
8 profiles, *Biometals* 29 (2016) 863–872. <https://doi.org/10.1007/s10534-016-9957-x>.

9
10 [10] B. D. Glisic, M. I. Djuran, Gold complexes as antimicrobial agents: an overview of different
11 biological activities in relation to the oxidation state of the gold ion and the ligand structure, *Dalton*
12 *Trans.*, 43 (2014) 5950-5969. <https://doi.org/10.1039/c4dt00022f>

13
14 [11] D.A. Safin, J. M. Frosta, M. Murugesu, The renaissance of 2,4,6-tris(2-pyrimidyl)-1,3,5-
15 triazine (TPymT) coordination chemistry, *Dalton Trans.* 44 (2015) 20287-20294.

16
17 <https://doi.org/10.1039/c5dt03435c>

18
19 [12] T. Marzo, D. Cirri, L. Ciofi, C. Gabbiani, A. Feis, N. Di Pasquale, M. Stefanini, T. Biver, L.
20 Messori, Synthesis, characterization and DNA interactions of [Pt₃(TpymT)Cl₃], the trinuclear
21 platinum(II) complex of the TpymT ligand, *J.Inorg. Biochem.* 183 (2018) 101–106.

22
23 <https://doi.org/10.1016/j.jinorgbio.2018.03.009>.

24
25 [13] J. Dickerhoff, N. Brundridge, S.A. McLuckey, D. Yang, Berberine Molecular Recognition of
26 the Parallel MYC G-Quadruplex in Solution *J. Med. Chem.* 64 (2021) 16205-16212.

27
28 <https://doi.org/10.1021/acs.jmedchem.1c01508>

29
30 [14] N.H. Campbell, N.H. Abd Karim, G.N. Parkinson, M. Gunaratnam, V. Petrucci, A.K. Todd, R.
31 Vilar, S. Neidle, Molecular Basis of Structure–Activity Relationships between Salphen Metal
32 Complexes and Human Telomeric DNA Quadruplexes, *J. Med. Chem.* 55 (2012) 209–222.

33
34 <https://doi.org/10.1021/jm201140v>.

35
36 [15] C. Bazzicalupi, M. Ferraroni, F. Papi, L. Massai, B. Bertrand, L. Messori, P. Gratteri, A.
37 Casini, Determinants for Tight and Selective Binding of a Medicinal Dicarbene Gold(I) Complex to
38

1 a Telomeric DNA G-Quadruplex: a Joint ESI MS and XRD Investigation, *Angew. Chem. Int. Ed.*
2 55 (2016) 4256-4259. <https://doi.org/10.1002/anie.201511999>.
3

4 [16] F. Guarra, T. Marzo, M. Ferraroni, F. Papi, C. Bazzicalupi, P. Gratteri, G. Pescitelli, L.
5 Messori, T. Biver, C. Gabbiani, *C. Dalton Trans.*, 47 (2018) 16132-16138.
6
7 <https://doi.org/10.1039/C8DT03607A>.
8

9
10 [17] a) U. Ryde, L. Olsen, K. Nilsson, Quantum chemical geometry optimisations in proteins using
11 crystallographic raw data, *J. Comp. Chem.*, 23 (2002) 1058-1070.
12
13 <https://doi.org/10.1002/jcc.10093>; b) J. Bergmann, E. Oksanen, U. Ryde, Combining
14 crystallography with quantum mechanics, *Curr. Opin. Struct. Biol.*, 72 (2021) 18-26.
15
16 <https://doi.org/10.1016/j.sbi.2021.07.002>; c) L. Cao, U. Ryde, Quantum refinement with multiple
17 conformations: Application to the P-cluster in nitrogenase *Acta Crystal. D*, 76 (2020) 1145-1156.
18
19 <https://doi.org/10.1107/S2059798320012917>; d) L. Cao, O. Caldararu, U. Ryde, Does the crystal
20 structure of vanadium nitrogenase contain a reaction intermediate? Evidence from quantum
21 refinement, *J. Biol. Inorg. Chem.*, 25 (2020) 847-861. <https://doi.org/10.1007/s00775-020-01813-z>;
22
23 e) L. Cao, O. Caldararu, A. C. Rosenzweig, U. Ryde, Quantum Refinement Does Not Support
24 Dinuclear Copper Sites in Crystal Structures of Particulate Methane Monooxygenase, *Angew.*
25 *Chem., Int. Ed.*, 57 (2018), 162–166. <https://doi.org/10.1002/anie.201708977>.
26
27 [18] N. H. Campbell, G. N. Parkinson, Crystallographic studies of quadruplex nucleic acids.
28 *Methods* 43 (2007) 252–263. <https://doi.org/10.1016/j.ymeth.2007.08.005>.
29
30 [19] W. Kabsch, XDS, *Acta Cryst.*, D66 (2010) 125–132.
31
32 <https://doi.org/10.1107/S0907444909047337>.
33
34 [20] A. Vagin, A. Teplyakov, MOLREP: an Automated Program for Molecular Replacement, *J.*
35 *Appl. Cryst.* 30, (1997) 1022–1025. <https://doi.org/10.1107/S0021889897006766>.
36
37 [21] G.N. Murshudov, A.A. Vagin, E.J. Dodson, Refinement of macromolecular structures by the
38 maximum-likelihood method, *Acta Crystallogr. D* 53 (1997) 240-255.
39
40 <https://doi.org/10.1107/S0907444996012255>.
41
42
43
44
45
46
47
48
49
50
51
52
53
54
55
56
57
58
59
60
61
62
63
64
65

- 1
2
3
4
5
6
7
8
9
10
11
12
13
14
15
16
17
18
19
20
21
22
23
24
25
26
27
28
29
30
31
32
33
34
35
36
37
38
39
40
41
42
43
44
45
46
47
48
49
50
51
52
53
54
55
56
57
58
59
60
61
62
63
64
65
- [22] M.D. Winn, C.C. Ballard, K.D. Cowtan, E.J. Dodson, P. Emsley, P.R. Evans, R.M. Keegan, E.B. Krissinel, A.G.W. Leslie, A. McCoy, S.J. McNicholas, G.N. Murshudov, N.S. Pannu, E.A. Potterton, H.R. Powell, R.J. Read, A. Vagin, K.S. Wilson, Overview of the CCP4 suite and current developments, *Acta Crystallogr D* 67 (2011) 235-242. <https://doi.org/10.1107/S0907444910045749>.
- [23] P. Emsley, B. Lohkamp, W.G. Scott, K. Cowtan, Features and development of Coot, *Acta Crystallogr* 66D (2010) 486-501. Doi: <https://doi.org/10.1107/S0907444910007493>.
- [24] Schrödinger Suite Release 2019-4, Schrödinger, LLC, New York, NY, 2019. A) Jaguar, v.10.3; b) Glide, v.8.2.
- [25] F. Furche, R. Ahlrichs, C. Hättig, W. Klopper, M. Sierka, F. Weigend, *Turbomole*, *WIREs Comput Mol Sci.* 4 (2014) 91–100. <https://doi.org/10.1002/wcms.1162>
- [26] A.T. Brunger, P.D. Adams, G.M. Clore, W.L. DeLano, P. Gros, R.W. Grosse-Kunstleve, J.S. Jiang, J. Kuszewski, M. Nilges, N.S. Pannu, R.J. Read, L.M. Rice, T. Simonson, G. L. Warren, *Crystallography & NMR system: A new software suite for macromolecular structure determination*, *Acta Crystallogr. D* 54 (1998):905–921. <https://doi.org/10.1107/s0907444998003254>; b) A.T. Brunger, Version 1.2 of the Crystallography and NMR system, *Nat Protoc* 2 (2007) 2728–33. <https://doi.org/10.1038/nprot.2007.406>.
- [27] a) N.S. Pannu, R.J. Read, Improved Structure Refinement Through Maximum Likelihood, *Acta Crystallogr Sect A Found Crystallogr* A52 (1996) 659–668. <https://doi.org/10.1107/S0108767396004370>; b) P.D. Adams, N.S. Pannu, R.J. Read, A.T. Brünger, Cross-validated maximum likelihood enhances crystallographic simulated annealing refinement, *Proc Natl Acad Sci U S A* 94 (1997)5018–5023. <https://doi.org/10.1073/pnas.94.10.5018>.
- [28] a) J. Tao, J.P. Perdew, V.N. Staroverov, G.E. Scuseria, Climbing the Density Functional Ladder: Nonempirical Meta-Generalized Gradient Approximation Designed for Molecules and Solids, *Phys Rev Lett* 91 (2003) 146401. <https://doi.org/10.1103/PhysRevLett.91.146401>; b) A. Schäfer, H. Horn, R. Ahlrichs, Fully optimized contracted Gaussian basis sets for atoms Li to Kr, *J Chem Phys* 97 (1992) 2571–2577. <https://doi.org/10.1063/1.463096>.

1 [29] a) K. Eichkorn, O. Treutler, H. Öhm, M. Häser, R. Ahlrichs, Auxiliary basis sets to
2 approximate Coulomb potentials, Chem Phys Lett 240 (1995) 283–289.

3
4 [https://doi.org/10.1016/0009-2614\(95\)00621-a](https://doi.org/10.1016/0009-2614(95)00621-a); b) K. Eichkorn, F. Weigend, O. Treutler, R.

5
6
7 Ahlrichs Auxiliary basis sets for main row atoms and transition metals and their use to approximate
8
9 Coulomb potentials, Theor. Chem. Acc. 97 (1997) 119–124.

10
11
12 <https://doi.org/10.1007/s002140050244>.

13
14 [30] S. Grimme, J. Antony, S. Ehrlich, H. Krieg, A consistent and accurate ab initio parametrization
15 of density functional dispersion correction (DFT-D) for the 94 elements H-Pu, J. Chem. Phys. 132
16 (2010) 154104 (19 pages). <https://doi.org/10.1063/1.3382344>

17
18
19 [31] S. Grimme, S. Ehrlich, L. Goerigk, Effect of the damping function in dispersion corrected
20 density functional theory, J. Comput. Chem. 32 (2011) 1456–1465.

21
22
23
24
25
26 <https://doi.org/10.1002/jcc.21759>.

27
28
29 [32] a) E.A. Allen, W. Wilkinson, Spectrochimica Acta, 28A (1972), 2257- 2262.

30
31
32 [https://doi.org/10.1016/0584-8539\(72\)80200-9](https://doi.org/10.1016/0584-8539(72)80200-9); b) D.R. Williamson, M.C. Baird, Gold-halogen
33 stretching frequencies, J. Inorg. Nucl. Chem. 34 (1972) 3393-3400. [https://doi.org/10.1016/0022-](https://doi.org/10.1016/0022-1902(72)80233-1)
34
35
36
37 [1902\(72\)80233-1](https://doi.org/10.1016/0022-1902(72)80233-1).

38
39 [33] PDB codes: 1KF1, 2HRI, 3CCO, 3QSC, 3QSF, 3UYH, 4DA3,4DAQ, 3SC8, 3TSE, 4FXM,
40
41 4G0F, 5DWX, 5DWW

42
43 [34] F.H. Allen, The Cambridge Structural Database: a quarter of a million crystal structures and
44 rising, Acta Cryst. B58 (2002) 380—388. <https://doi.org/10.1107/S0108768102003890>. The CSD
45
46 version used in this work was updated in 2021.

47
48
49 [35] M. Savastano, C. García-Gallarín, M.D. López de la Torre, C. Bazzicalupi, A. Bianchi, M.
50
51 Melguizo, Anion Complexes with Tetrazine-Based Ligands: Formation of Strong Anion– π
52
53 Interactions in Solution and in the Solid State, Coord. Chem. Rev. 397 (2019) 112–137.

54
55
56
57
58 <https://doi.org/10.1021/acs.inorgchem.6b01138>.

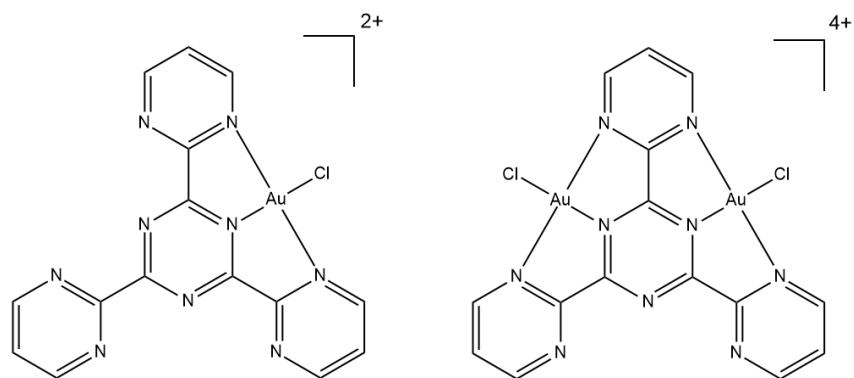
59
60
61
62
63
64
65

Captions to illustrations

1
2
3
4
5 Figure 1. Chemical structure of the gold(III) complexes obtained by reaction of the TpymT- α
6
7 ligand. Both complexes coordinate exogenous chloride ligands.
8

9
10 Figure 2. Melting plot of G4 alone (■) ($CG_4 = 9.90 \times 10^{-6}$ M) and G4 with product (I) (●), or
11
12 TpymT- α ligand (▲), $C_{\text{product (I)}}/CG_4 = C_{\text{ligand}}/CG_4 = 3$, NH_4OAc 0.1 M, $pH = 7.0$.
13

14
15 Figure 3. a) Column of stacked G-quadruplexes in the crystal packing of the $Tel_{24}/[(TpymT-$
16
17 $\alpha)AuCl]$ crystal structure. K^+ ions are shown as purple spheres; b-e) Details of each single position
18
19 of the $[(TpymT-\alpha)AuCl]$ gold-complex stacked on the 3'-end G-tetrad. Color code for the carbon
20
21 atoms of the four approximately coplanar disordered $[(TpymT-\alpha)AuCl]$ molecules stacked on the
22
23 3'-end G-tetrads defining the binding site: $[(TpymT-\alpha)AuCl]$ -C (by element), $[(TpymT-\alpha)AuCl]$ -D
24
25 (green), $[(TpymT-\alpha)AuCl]$ -E (orange red), $[(TpymT-\alpha)AuCl]$ -F (orange), symmetry related
26
27 $[(TpymT-\alpha)AuCl]$ molecules (black).
28
29
30
31
32
33
34
35
36
37
38
39
40
41
42
43
44
45
46
47
48
49
50
51
52
53
54
55
56
57
58
59
60
61
62
63
64
65

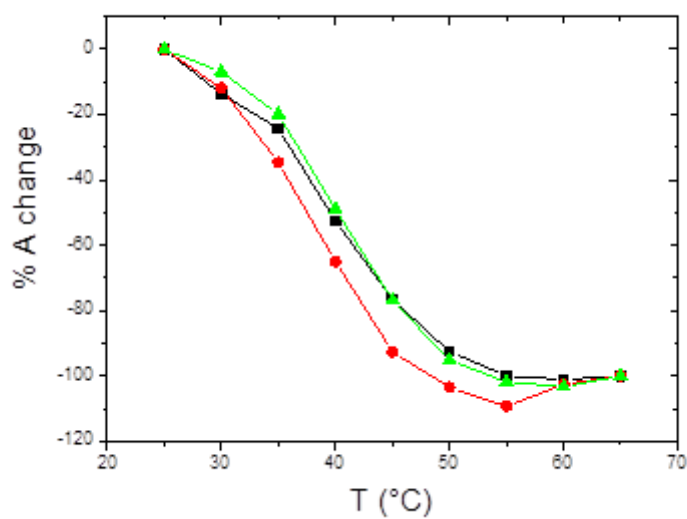


International Journal of Biological Macromolecules

Damiano Cirri, Carla Bazzicalupi, Ulf Ryde, Justin Bergmann, Francesca Binacchi, Alessio

Nocentini, Alessandro Pratesi, Paola Gratteri, Luigi Messori

Figure 1.



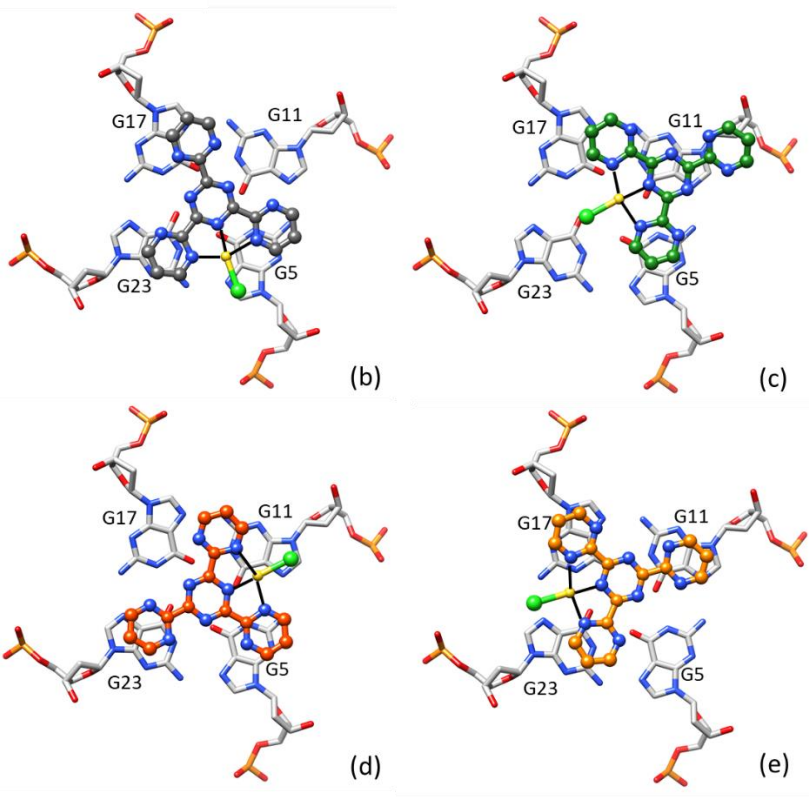
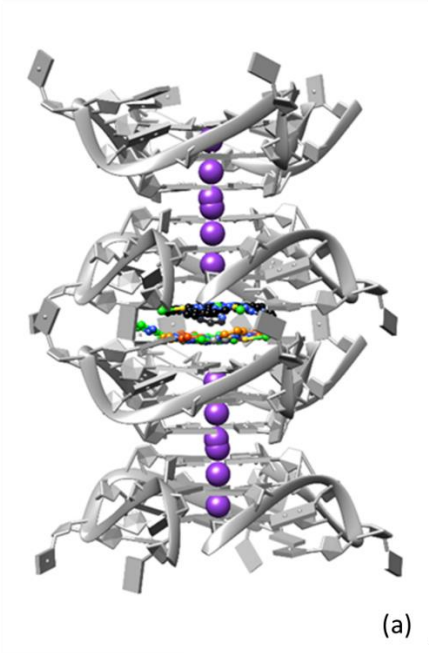
International Journal of Biological Macromolecules

Damiano Cirri, Carla Bazzicalupi, Ulf Ryde, Justin Bergmann, Francesca Binacchi, Alessio

Nocentini, Alessandro Pratesi, Paola Gratteri, Luigi Messori

Figure 2.

1
2
3
4
5
6
7
8
9
10
11
12
13
14
15
16
17
18
19
20
21
22
23
24
25
26
27
28
29
30
31
32
33
34
35
36
37
38
39
40
41
42
43
44
45
46
47
48
49
50
51
52
53
54
55
56
57
58
59
60
61
62
63
64
65



International Journal of Biological Macromolecules

Damiano Cirri, Carla Bazzicalupi, Ulf Ryde, Justin Bergmann, Francesca Binacchi, Alessio Nocentini, Alessandro Pratesi, Paola Gratteri, Luigi Messori

Figure 3.



Computationally enhanced X-ray diffraction analysis of a gold(III) complex interacting with the human telomeric DNA G-quadruplex. Unravelling non-unique ligand positioning

Damiano Cirri^a, Carla Bazzicalupi^{b,*}, Ulf Ryde^{c,*}, Justin Bergmann^c, Francesca

Binacchi^a, Alessio Nocentini^d, Alessandro Pratesi^a, Paola Gratteri^{d,*}, Luigi Messori^b

a Department of Chemistry and Industrial Chemistry, University of Pisa, Via G. Moruzzi 13, 56124 Pisa, Italy.

b Department of Chemistry “Ugo Schiff”, University of Florence, Via della Lastruccia 3-13, 50019 Sesto Fiorentino, Italy.

c Division of Theoretical Chemistry, Lund University, Chemical Centre, P. O. Box 124, SE-221 00 Lund, Sweden

d Department NEUROFARBA – Pharmaceutical and Nutraceutical Section and Laboratory of Molecular Modeling Cheminformatics & QSAR, University of Florence, Via U. Schiff 6, 50019 Sesto Fiorentino, Florence, Italy.

Highlights

- G4 can be characterized by non-unique positioning of ligands on the guanine tetrad
- crystallographic refinement enhanced with QM/MM calculations
- mononuclear gold complex stacked at the 3'-end G-tetrad of the human telomeric DNA



Click here to access/download
MethodsX
methodsx.docx

